Preprints (www.preprints.org) | NOT PEER-REVIEWED | Posted: 17 March 2017 doi:10.20944/preprints201703.0140.v1

Article

Efficiency Increase of Vibratory Energy Harvesting Circuits by Multi-Harvester Strategy Design

Javier Ortiz [1], Josu Etxaniz [1,*], Nieves Murillo [2], Joseba Zubia [3], and Gerardo Aranguren [1]

[1] Electronic Design Group, Engineering Faculty, University of the Basque Country, Bilbao, Spain
[2] Industry & Transport Division, TECNALIA, San Sebastian, Spain
[3] Applied Photonics Group, Engineering Faculty, University of the Basque Country, Bilbao, Spain
* Correspondence: josu.etxaniz@ehu.es; Tel.: +34-94601-3992

Abstract: Since the requirements in terms of power of the electronic applications range wide, the developed Energy Harvesting (EH) systems limit their availability to the less power demanding applications. However, this paper focuses on increasing the energy levels collected in the EH system so that it can be included in more demanding applications in terms of power. Therefore, an electronic system capable of grouping many single harvesting channels into one single system is analyzed in this paper. This multi-harvester electronic system is able to manage efficiently the energy collected by multiple vibratory transducers. The paper includes a comparison of its performance against some of the State-of-the-Art EH energy management circuits that interface the transducers. The method employed to demonstrate the intrinsic efficiency of each of the electronic circuits tested was based on experimental tests, where the average power transferred from several identical and simultaneous electric sources to a single storage element was measured. It was found out that only one energy management circuit was able to increase the transferred energy in a linear way while new input electric sources were added.

Keywords: Energy Harvesting; energy management circuit; kinetic energy; vibratory transducer.

---

1. Introduction

The energy harvesting (EH) technologies are gathering more and more interest in the academia and industry. Many monitoring and control applications require wireless sensor and actuator networks. The networks are composed of independent nodes that are not plugged to electric power supply and need independent power sources. Thus, it is mandatory to provide an autonomous power source to each node of the network so that their useful life is as long as possible.

Several sources to obtain and convert electrical energy are in the limelight. For example, ambient energy, as light, thermal gradients, kinetic energy or radiofrequency (RF) energy, is transformed into electrical energy. Kinetic sources applied to piezoelectric transducers [1] are in the spotlight of this research since mechanic vibrations are present in a number of useful locations, such as transport vehicles, electromechanical machines or just walking [2, 3].

There are three primary transduction mechanisms that convert mechanical energy into electrical energy: electromagnetic (EM) [4, 5], electrostatic (ES) [6-8] and piezoelectric (PE) [9-11]. The first mechanism is based on Faraday's induction law. Electromagnetic coils, usually large, produce power levels that range from 20 μW to 2000 μW [12] but the output voltage is low (<1 V) and they require additional conversion stages. Next, the electrostatic devices that use a variable capacitor to harvest energy produce significantly lower power levels (10-40 μW) than those coming from electromagnetic devices [13-15]. The last mechanism, the piezoelectric transduction, offers suitable output voltages of up to 20 V. Piezoelectric transducers are well suited for miniaturization. However, they show extremely high output impedances and, hence, the levels of output currents in the range of microamperes provide levels of power up to microwatts.

The power levels achieved for vibration energy harvesting are summarized in Table 1, which is arranged considering the type of transduction.

Table 1. Power Levels Achieved in Some Vibrational Energy Harvesters. *P* is the power achieved, *f* is the frequency of the vibrations, *a* is the acceleration of the transducers and *Pd* is the power density.

Type	P (μW)	F (Hz)	a (m/s²)	Pd (μW/mm³)
EM [12]	2000	100	1.0	0.04
EM [16]	1500	60	1.0	0.05
ES [17]	24	30	10	0.015
ES [18]	8	50	8.8	0.21
PE [19]	375	120	2.5	0.18
PE [20]	160	80	2.3	0.25

However, the energy requirements of electronic systems depend upon the specific application they are meant to. It may happen that the amount of voltage or electronic power given by the EH system does not satisfy the conditions of many applications, as, for instance, in wireless sensor networks.

Nowadays, autonomous self-powered wireless sensor networking is one of the scopes in EH. Despite there are relevant improvements in piezoelectric materials and transduction properties [21-26], there can be found some applications of autonomous wireless sensors that cannot meet the required minimum power specifications. However, the small energy harvested limits the consumption of sensors. The most common way to reduce consumption is to decrease the sampling rate and, therefore, assume that some loss of relevant data could happen. But the reduction of the performance of the system cannot be acceptable in many applications.

Therefore, to prevent such situations, the efficiency of the vibratory energy harvester circuit must be enhanced. The path to explore in this research is the design and implementation of a multi-harvester system by using several interconnected harvesters. This solution increases the efficiency of the EH system and offers higher power levels.

Furthermore, the high patentability of EH technologies as well as their availability to substitute the batteries of low-consumption electronic devices make the EH technologies more attractive. The literature on EH is mainly focused on building prototypes to power electronic devices. The size of the EH prototypes ranges from nanometers to micrometers. The proposals in the literature increase the application range of EH technologies to systems that consume just a few mW. However, this paper introduces research on EH electronic systems that use multiple piezoelectric transducers to collect energy. More specifically, kinetic sources with piezoelectric transduction applied to multiple sources are considered from the point of view of the energy efficiency in the electronic management stage.

Section 2 provides a general schematic of an EH system that focuses on the energy management block and the EH circuits available. Section 3 focuses on the use of multiple harvesters to increase the power given to the electronic system. Section 4 introduces the experimental setup used to compare EH circuits and discusses the results of the harvested energy with some EH circuits. Section 5 analyzes the intrinsic efficiency of the EH electronic circuits. Finally, the last section summarizes the conclusions drawn.

2. Energy Harvesting Circuits

A typical energy harvester system consists of several subsystems, which include energy transducers, energy management hardware and energy storage, which provides energy to the electronic application under suitable and stable voltage specifications. A generic vibratory energy harvester system schematic is shown in Figure 1.

 doi:10.20944/preprints201703.0140.v1

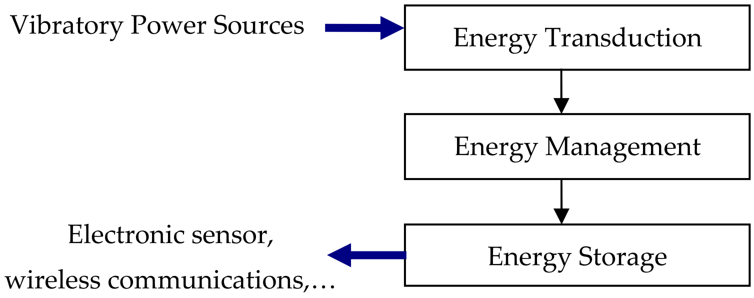

Figure 1. Schematic of a generic vibratory energy harvester system.

Given the ultralow current levels generated by the piezoelectric effect in the range of tens of microwatts, it is essential that the electronic interface or circuit for power management can optimize the collection and conversion processes. In most applications, the generated average power is not high enough to power any electric load, not even the least power demanding sensor circuits, with its data logger or wireless communication system. Hence, the mode of operation must be discontinuous and must alternate the phase that charges the storage element, which can be done using an element such as a bulky capacitor or using the phase that feeds the electric load.

Energy storage can be implemented by a rechargeable battery or a capacitor. The latter is more advantageous because of the simplicity of the circuits to charge it and discharge it.

The fundamentals of electronic circuits for EH are introduced in [27]. Generally speaking, the simplest circuit for energy management is the diode full-bridge rectifier, Figure 2(a), however, its efficiency is extremely dependent on the electrical load. Attempts have been made to design circuits to improve the diode full-bridge performance. There are two types of proposals for this issue.

The first option was investigated by a group of researchers [28-30] who developed a nonlinear technique called Synchronized Switch Harvesting on Inductor (SSHI), which is based on commuting the piezoelectric transducer over an inductor at the moment of maximum electric energy harvested in the piezoelectric transducer. This technique can be implemented with many configurations, such as parallel SSHI, series SSHI (Figure 2 (b)), Synchronous Electric Charge Extraction (SECE) (Figure 2 (c)) and similar configurations that replace the inductor with a transformer. It is interesting to note that these techniques are derived from the Synchronized Switch Damping (SSD) method, which is an electrical technique developed to address the problem of vibration damping on mechanical structures.

The second type of circuits to improve the low efficiency of the standard diode full-bridge includes inserting a DC/DC converter between the diode full-bridge rectifier and the store capacitor (Figure 2 (d)). The use of a bulky capacitor (C_p) as a buffer to store energy poses a problem in that the capacitor cannot intrinsically ensure optimal power generation if it is directly connected to the rectifier output. With the inclusion of the DC/DC converter, the rectifier is forced to work at its optimal operating point, with a voltage in the rectified output V_{rect} equal to half of the open-circuit voltage V_p across the piezoelectric electrodes.

Preprints (www.preprints.org) | NOT PEER-REVIEWED | Posted: 17 March 2017 doi:10.20944/preprints201703.0140.v1

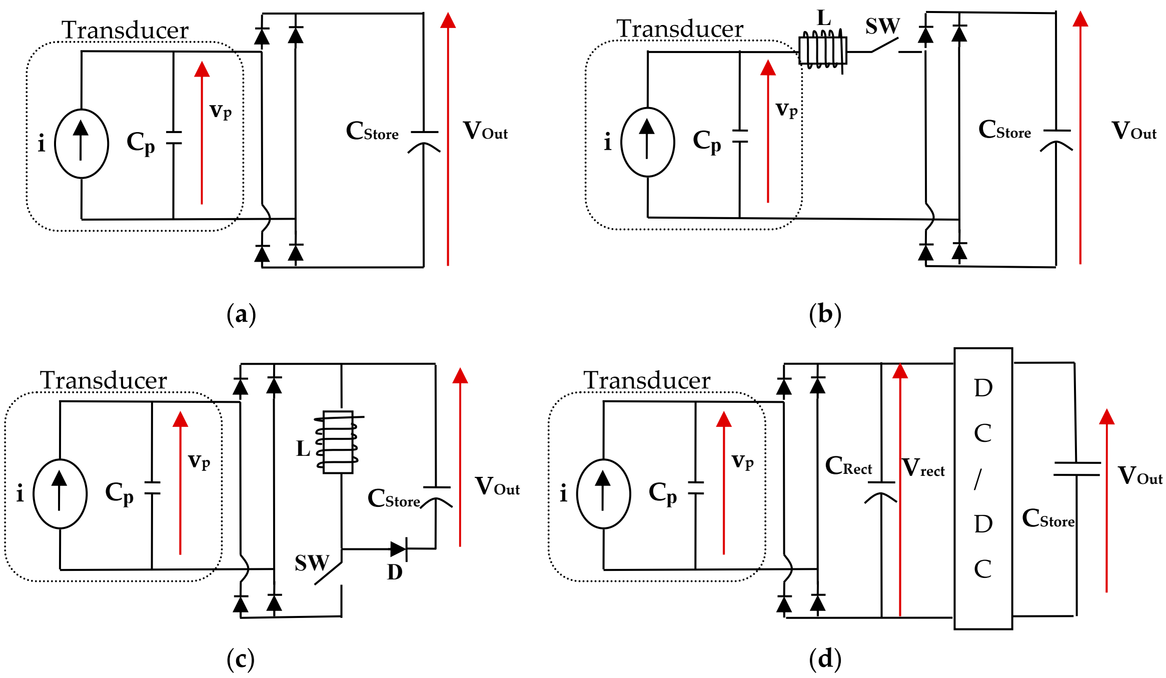

Figure 2. Simplified schemes of the common types of energy harvesting circuits. (a) Diode full-bridge rectifier (b) series SSHI (c) SECE (d) Adaptive DC/DC.

Therefore, the DC/DC converter must not only regulate its output voltage but also offer optimal input impedance to the rectifier. However, in many cases, the amplitude of the vibrations and, hence, the V_P voltages generated by the piezoelectric transducer are not constant value. However, the adjustment of the converter's duty cycle with feedback control maximizes the power of the system. The feedback control implies the use of circuits with extremely high consumption requirements. An adaptive energy-harvesting circuit with low power dissipation is presented in [28]. There, an ultralow-power analog controller eases the control and, as a result, the overall efficiency of the circuit is about 50% when the output power is greater than 0.5 mW. Several power optimization approaches for piezoelectric electrical generators available in literature propose simplifications that lead to the replacement of closed-loop circuits to open-loop circuits. Ottman et al. [29] introduced a step-down DC/DC buck converter. There, an optimal fixed duty cycle can be determined to maximize the harvested power for a given frequency of mechanical excitation. The optimal duty cycle for maximum power transfer turns to be almost constant when the amplitude of the mechanical excitation is above a threshold, and is highly variable for amplitudes below that value. Lefeuvre et al. [30] introduced the control of a buck-boost converter to track the generator's optimal working points. In this case, the duty cycle is determined as a function of the voltage of the battery to be charged and as a function of the maximum expected value of the converter input voltage. Next, the inductor and switching frequency can be determined such that the input resistance of the converter equals the matching load resistance of the piezoelectric device. In a similar way, Yu et al. [31] introduced the same buck-boost topology for the impedance matching block and added a bleed-off circuit in the energy storage stage.

The drawback of these open loop solutions is that when operating with fixed values of the duty cycle, the results are successful only when the input voltage is within a fixed range of input voltages. Nevertheless, a converter could be designed to fix the output voltage of the rectifier at the optimal value for applications where the vibration amplitudes are known and are essentially constant.

Several attempts have been made to implement optimized harvesting circuit designs with closed-loop control as a digital CMOS chip. For instance, a time-multiplexing mechanism for a maximum power point is proposed by Chao el. al. [32]. The output of the piezoelectric film is periodically disconnected from the application and connected to a vibration tracking unit to

Preprints (www.preprints.org) | NOT PEER-REVIEWED | Posted: 17 March 2017 doi:10.20944/preprints201703.0140.v1

measure the maximum voltage and to regulate the step-down converter. The power utilization efficiency of the overall platform is greater than 50%.

An Integrated Circuit (IC) designed for auto-harvesting applications with high-impedance transducers, the LTC3588-1 [33], can be found in the market of electronic devices (see Figure 3). The architecture of the IC-based circuit is similar to the adaptive DC/DC one presented in the Figure 2d.

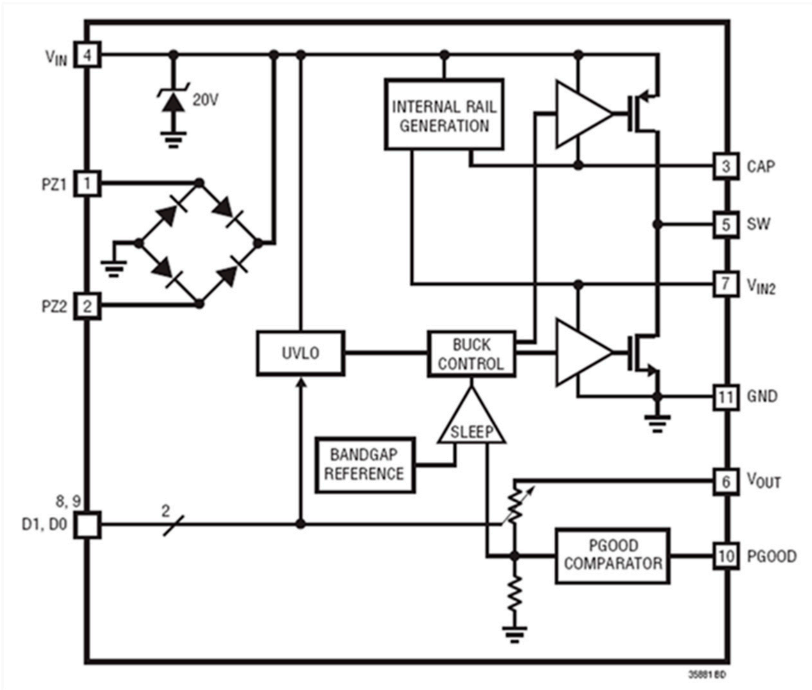

Figure 3. Block diagram of the LT3588-1 IC (Courtesy of Linear Technologies)

3. Multiple Transducers and Multiple Energy Management Circuits

Certain applications require more energy than the one given by a single energy harvesting system. In these applications and under certain conditions, in particular when there are no restrictions regarding the available volume that can be occupied, it is possible to attain higher power by means of adding multiple transducers. There are two ways of connecting several piezoelectric transducers to an energy management circuit: series, as shown in Figure 4(a), and parallel, as shown in Figure 4(b). Lin et al. [34] describe many possibilities for using several piezoelectric transducers connected in serie ways. In the former, the power level increases with the voltage amplitude in the electrodes of the transducers, and in the latter, it increases with the amplitude of the output currents. When working under low levels of vibration, the higher output voltage given by the series connection leads to the advantage of higher probability of reaching the minimum threshold voltage at the input rectifier stage. However, the individually generated voltages must be in phase in both types of connections such that they do not cancel when being added to ensure that the performance is acceptable. This condition can only be satisfied when the transducers are placed together on areas under similar mechanical excitation. Therefore, the restriction on connecting multiple transducers limits their use to well-defined areas where mechanical excitations are known with certainty.

Regardless of these restrictions, the most efficient solution is to maximize the harvesting of vibratory energy from each transducer and to connect each transducer to an energy management circuit. To complete the whole circuit, all energy management circuits transfer the collected power to the single energy storage device as the diagram block shows in Figure 4(c). In the next section, the selected energy management circuits will be tested by working connected to multiple transducers simultaneously, as shown in Figure 4(c).

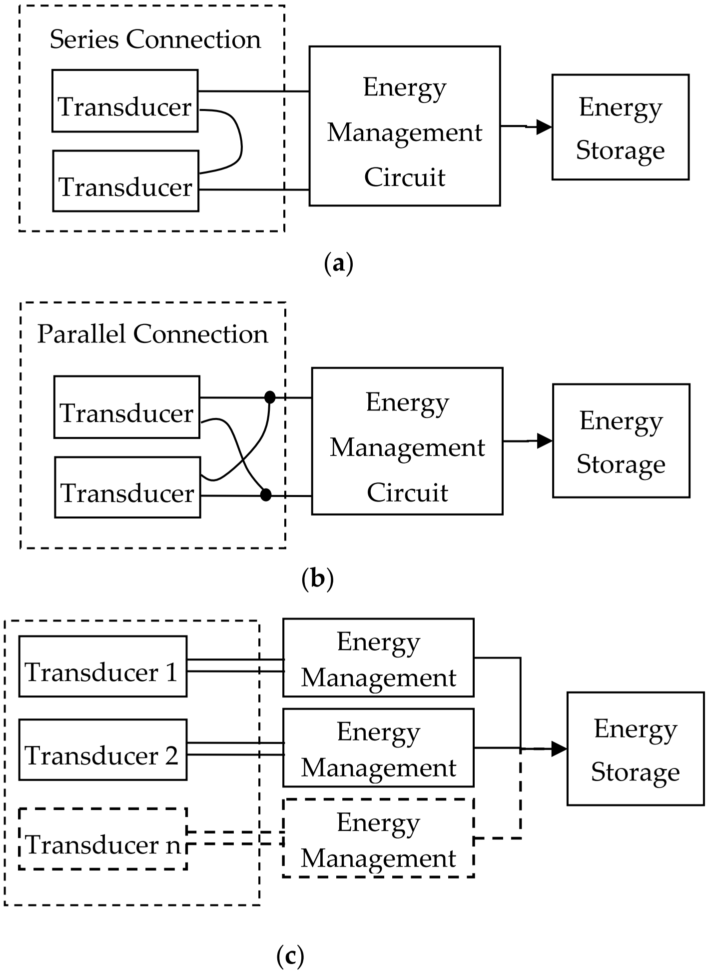

Figure 4. Three configurations with multiple transducers: (a) interconnecting each other in series mode to an energy management circuit (b) the same in parallel mode (c) connecting each transducer to an energy management circuit and these circuits connected to an energy storage circuit.

4. Experimental Setup to Compare EH Circuits

In the two preceding sections, the functional description and characteristics of the main EH circuits were introduced. In addition, it was discussed how the eventual need for a growing collection of energy led to the use of multiple transducers and circuits. In this section, the details of the experimental set-up for comparing EH circuits are given. Then, a set of tests was performed to compare the efficiency of these energy management circuits. The primary goal of the set of tests was to measure the efficiency of each one of the EH circuits. Then, the circuits were grouped to work in parallel to harvest higher levels of power. Therefore, each circuit was connected to other identical circuits to form groups of two, three and four energy management circuits working in parallel.

Thus, four types of circuits were selected and grouped on the workbench panels, as shown in Figure 5: the diode full-bridge (used as the reference in this test), the series SSHI, the SECE and the circuit based on the integrated circuit LTC3588-1 (hereinafter referred to as IC-based). Each one of the energy harvester circuits (transducer plus energy management) represents one channel.

Preprints (www.preprints.org) | NOT PEER-REVIEWED | Posted: 17 March 2017 doi:10.20944/preprints201703.0140.v1

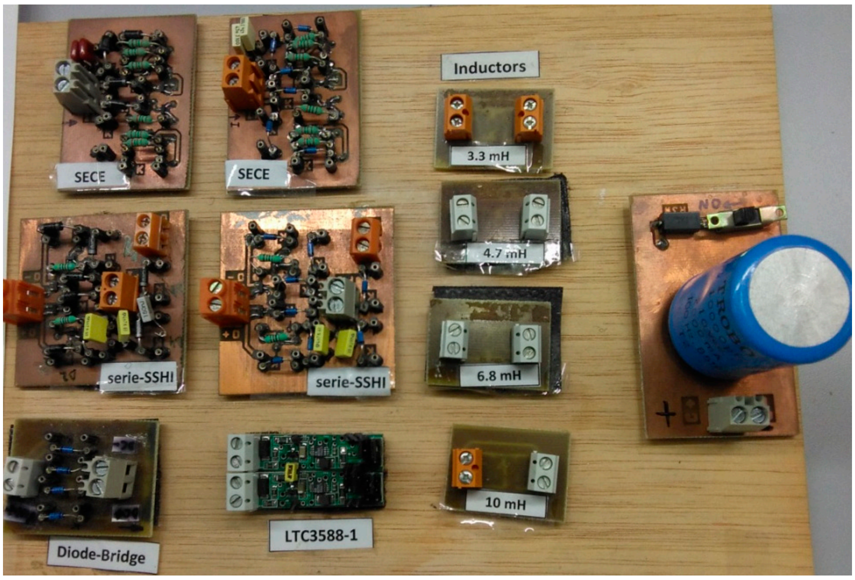

Figure 5. Workbench panel to testing EH circuits.

During the tests, one, two, three and four channels of each type were connected in parallel, as explained below:

- The diode full-bridge circuits are connected directly to the store capacitor (Figure 6a).
- The series SSHI circuits are fully independent and they only share the output capacitor (Figure 6b). Moreover, each circuit includes a self-powered switching subsystem.
- The SECE circuits, when grouped, share the three main output elements of the converter: capacitor, inductance and diode (Figure 6c). Each circuit includes a self-powered switching circuit to connect the transducer-rectifier stage and the common output stage.
- The IC-based circuits are connected each other sharing a common terminal to the output capacitor (C_{Store}) as well as sharing a common terminal connected to the small intermediate capacitor (C_{rect}) at the output of the internal rectifier stage (Figure 6d).

Preprints (www.preprints.org) | NOT PEER-REVIEWED | Posted: 17 March 2017 doi:10.20944/preprints201703.0140.v1

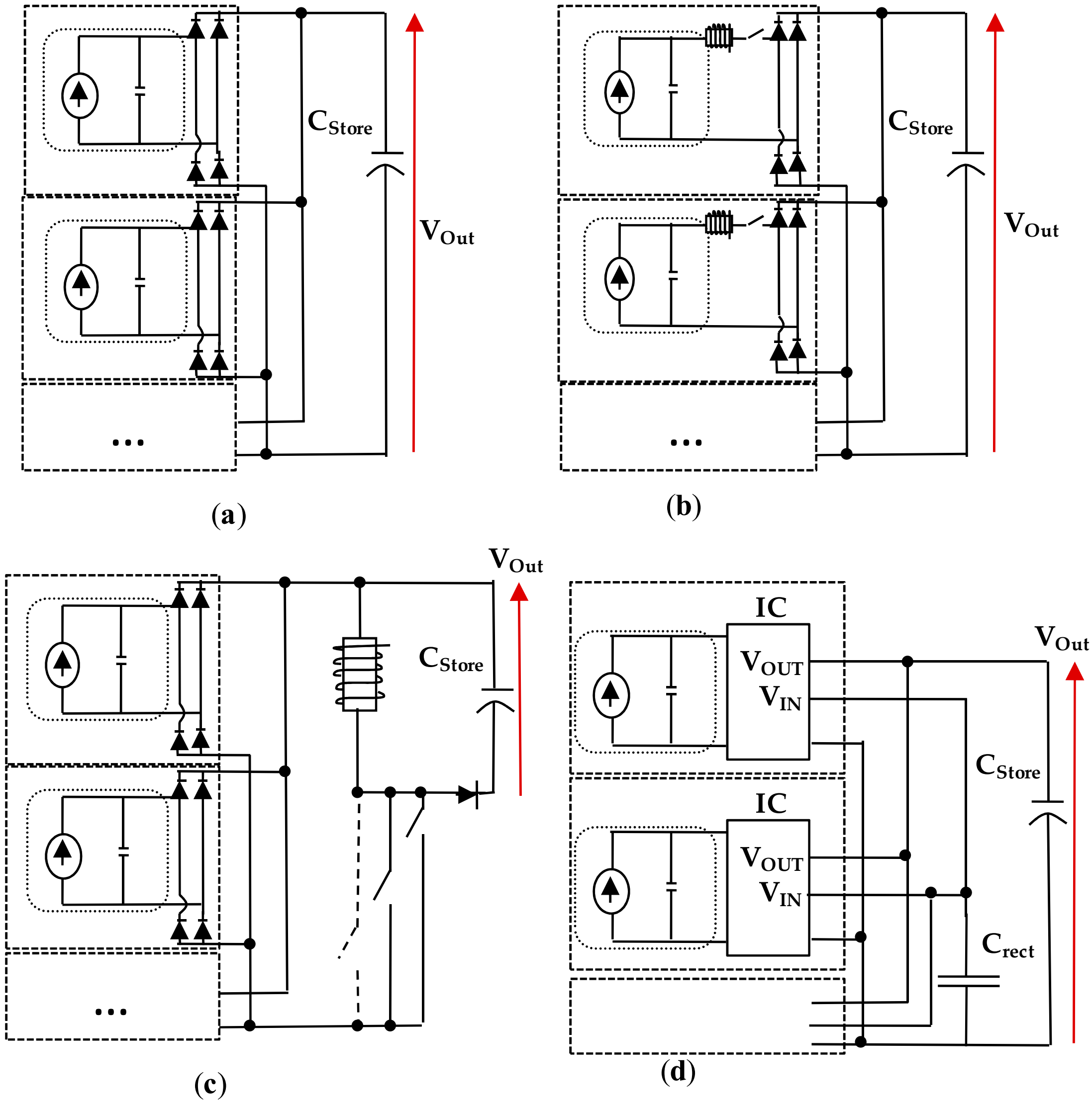

Figure 6. Schemes of the implemented multiple harvester circuits. (a) Diode full-bridge rectifier (b) series SSHI (c) SECE (d) IC-Based.

The tests consisted of measuring the time that a 10 mF capacitor needs to be charged within some specific range of electric voltage. The value of the capacity was chosen because it can store the amount of energy that can feed satisfactorily a wireless node type load. The energy stored in a capacitor of C capacity when charging it from V_1 initial voltage to V_2 end voltage can be obtained from the well-known Equation (1).

$$E = \frac{1}{2}C(V_2^2 - V_1^2), \qquad (1)$$

The resulting average power is defined by Equation (2). It can be calculated by just measuring the time of charge. Then, the results obtained in several types of circuits can be easily compared.

$$P_{avg} = \frac{E}{t} \qquad (2)$$

Initially, the piezoelectric transducer was substituted by an electric circuit based on the simplified Thevenin equivalent model of the transducer, as shown in Figure 7. The use of the equivalent circuit is a big advantage due to its simplicity and convenience when carrying out the tests. The Thevenin equivalent circuit was built considering the data included in the data-sheet of the manufacturer of the transducer, more specifically the i_P current and the internal capacity C_P (150

Preprints (www.preprints.org) | NOT PEER-REVIEWED | Posted: 17 March 2017 doi:10.20944/preprints201703.0140.v1

nF). The circuit was previously validated with the data obtained from the preliminary trials performed with the M8528-P2 MFC [35] transducer, a D_{31} mode type of Macro Fiber Composite, which is attached to a substrate material (FR4) 100x30x1mm thick forming a cantilever beam, as shown in Figure 8.

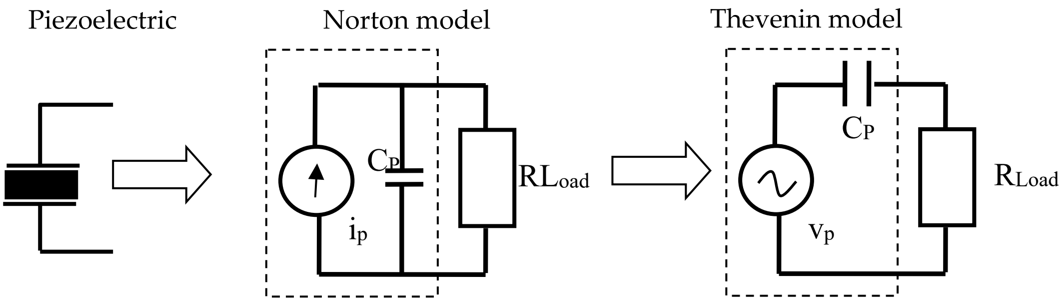

Figure 7. Schematic of the simplified Norton and Thevenin equivalent models of the piezoelectric transducer.

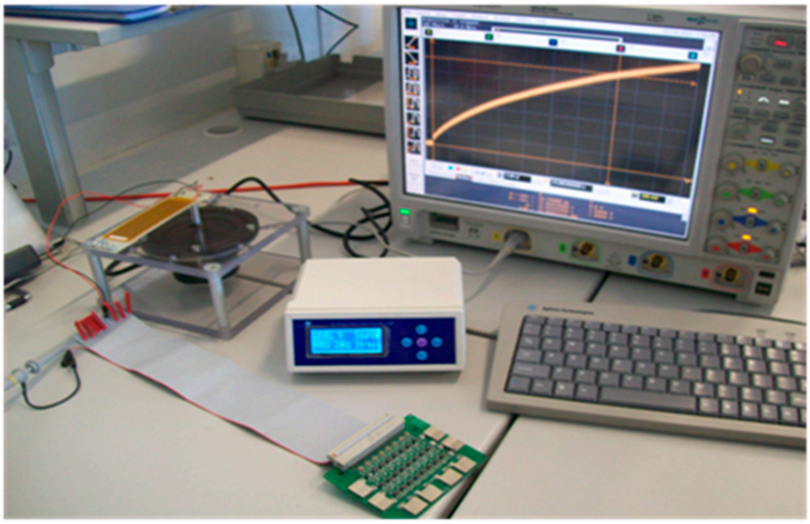

Figure 8. Set-up of the preliminary trials performed with the M8528-P2 MFC type piezoelectric transducer for its electric characterizing and subsequent validation of the Thevenin equivalent circuit.

The Thevenin equivalent circuit was implemented with a series connected function generator, 150 nF ceramic capacitor and a resistive load. The sinusoidal voltage of the known amplitudes ($V_{oc\text{-}pp}$) for each one of the situations considered (0.5 g_{rms}, 1.0 g_{rms} and 1.5 g_{rms}) was generated. It was applied to the input of the circuit. The load resistance was changed from 10 kΩ to 1 MΩ for each one of the voltage amplitudes considered. The peak-to-peak voltage drops in the load were measured, and they were compared with the results obtained in the trials to characterize the transducer.

To start with, it was determined the resonance frequency of the piezoelectric bender (piezoelectric transducer stuck to the carbon fiber piece). It was approximately 20 Hz. Later on, the peak-to-peak voltage drops generated were measured. The voltage drops were generated by the piezoelectric transducers under harmonic vibratory acceleration forces of 0.5 g_{rms}, 1.0 g_{rms} and 1.5 g_{rms}. First, the open-circuit peak-to-peak voltage drops ($V_{oc\text{-}pp}$) were measured with no load connected. The measured values for each situation were 10 V, 25 V and 36 V, respectively. Next, the trials were repeated with the electrodes of the transducer connected to electronic loads that ranged from 10 kΩ to 1 MΩ. These data were considered as reference and they were compared with the data obtained from the trials with the Thevenin equivalent circuit.

Preprints (www.preprints.org) | NOT PEER-REVIEWED | Posted: 17 March 2017 doi:10.20944/preprints201703.0140.v1

To finish the validation trials, the circuit was simulated with PSIM software [36]. Figure 9 summarizes the voltage drops obtained in the three types of trials, i.e., the results of the measurement in the equivalent circuit, the simulation of the piezoelectric transducer and, the measurements in the transducer.

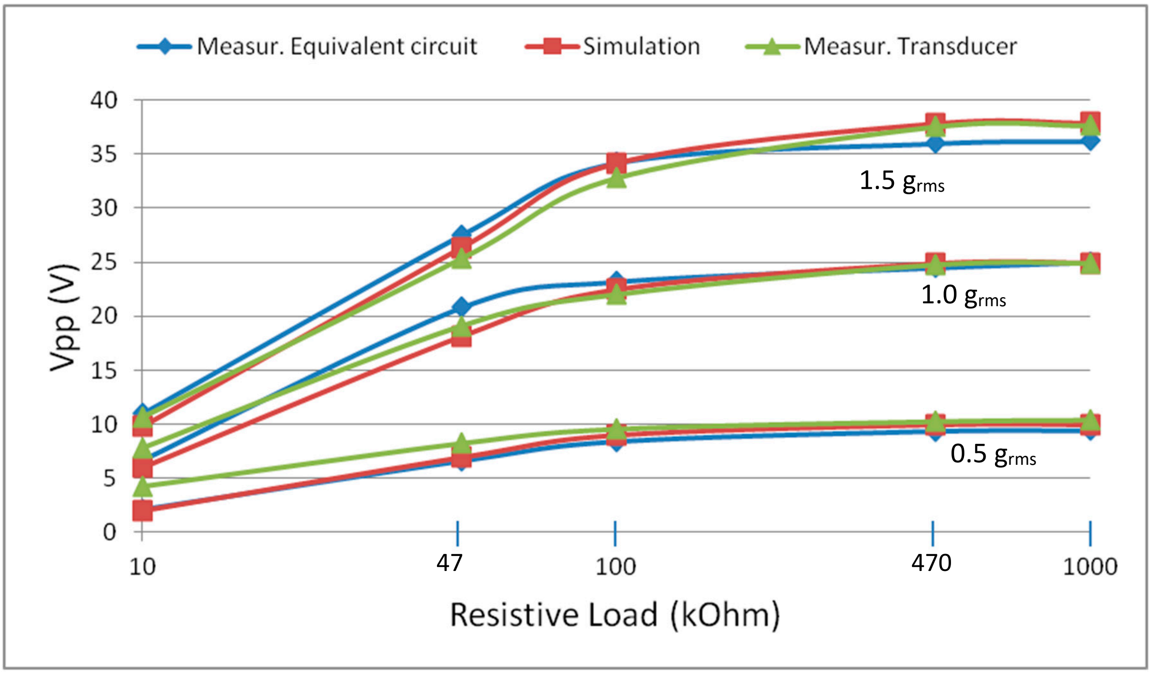

Figure 9. Set of results of the trials for the experimental validation of the Thevenin equivalent circuit of the M8528-P2 MFC piezoelectric transducer.

The results showed some slight differences among the voltage drops measured in the actual Thevenin circuit and those in the piezoelectric transducers. On the other hand, there was almost no difference between the actual and the simulated circuit, because the C_P capacitor was modeled with 15% tolerance.

After that, the comparative tests of the energy management circuits started. They were carried out with the simplified Thevenin equivalent circuit. The input signal for the tests was obtained from the function generator (20 V_{pp} and 20 Hz). During the tests, such signal was connected to each one of the EH circuits under test. The test series were performed for each one of the circuit types, and they were connected in parallel in groups of two, three and four circuits. Figure 10 shows the configuration of the test for the case of four simultaneous energy management circuits.

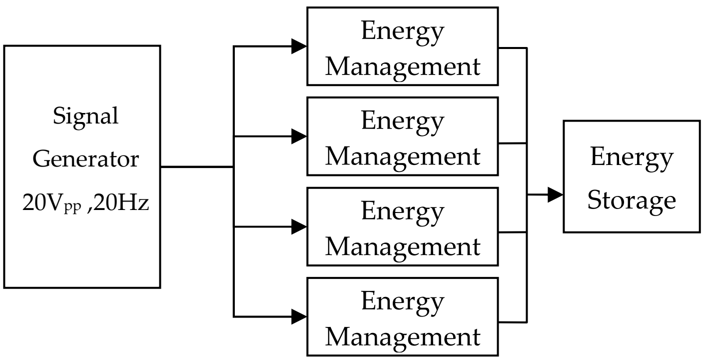

Figure 10. Test configuration for the case of four simultaneous channels.

 doi:10.20944/preprints201703.0140.v1

The tests consisted of measuring the time it takes to charge, from 0 V to 1.8 V, a single 10 mF capacitor connected to the output of the energy management circuit. Figure 11 depicts the time it took the operation with the four types of EH circuits under test, i.e., with the full diode-bridge, the series SSHI, the SECE and the IC-based circuit. Moreover, each type of EH circuit was tested individually and operating two and four of them in parallel, named channels.

The voltage change from 0 V to 1.8 V takes longer to the IC-based circuit proposed in this paper than to the series SSHI and SECE circuits. However, the IC-based circuit gives charge to the capacitor faster than the series SSHI and SECE circuits when considering two or four simultaneous channels.

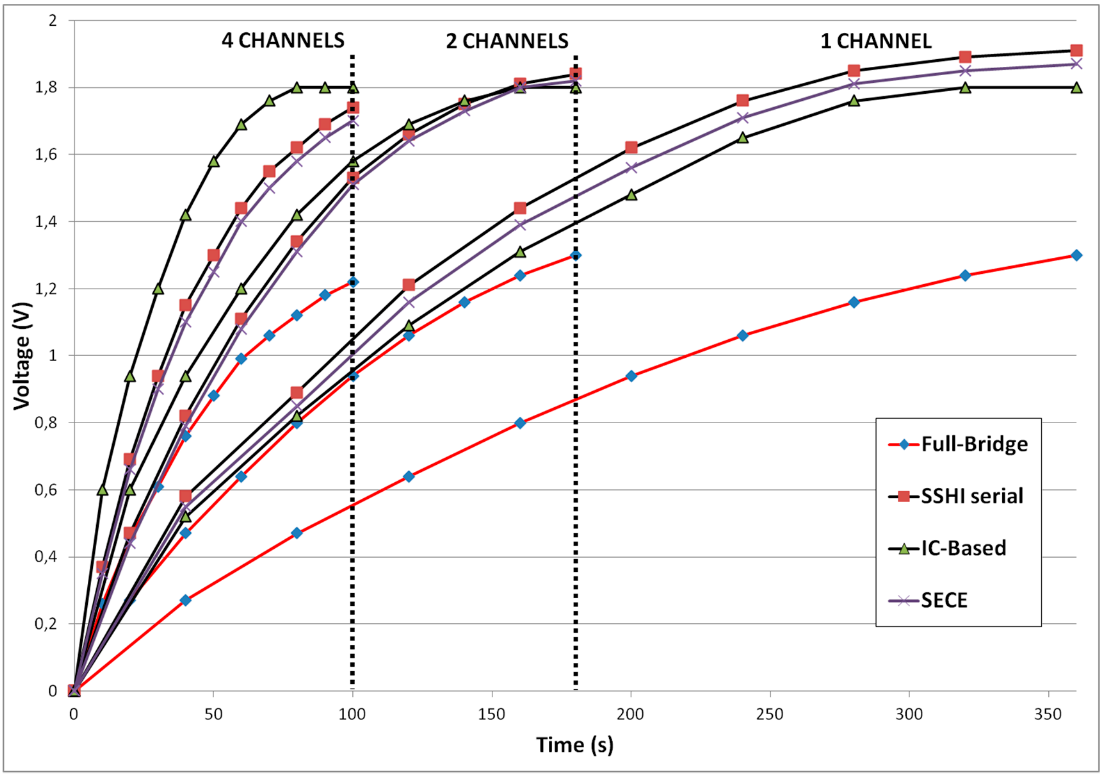

Figure 11. Output voltage versus time curves for the four types of circuits using (results for three channels are not drawn for the sake of clarity of the figure).

Figure 12 shows the average power transferred to the capacitor load for each one of the four cases and types of circuit considered here. It can be seen the clear linear evolution of the transferred average power when the IC-based energy management circuit is considered.

Preprints (www.preprints.org) | NOT PEER-REVIEWED | Posted: 17 March 2017 doi:10.20944/preprints201703.0140.v1

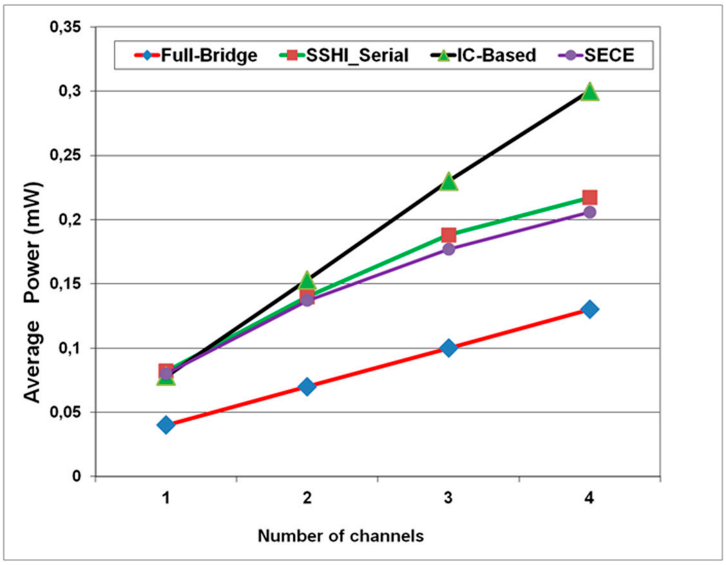

Figure 12. Average power (measured in mW) for the four EH circuits under test when using one to four channels simultaneously.

The data shown in the families of curves of Figure 11 clearly indicates how the IC-based circuit compared to the other circuits, charges the capacitor more quickly for the case of two and four harvesters connected in parallel. When calculating the average power transferred to the capacitor the average power grows almost linearly in the case of the IC-based circuit. Figure 12 proves that, for the case of two, three and four harvesters connected in parallel, the slope of the average power curve is almost constant in the case of the IC-based.

Generally speaking, when the amount of circuits connected in parallel grows, the slope of the actual average power of any parallel association shows a certain decrease from the theoretical linear value. Even with a certain amount of parallel circuits, the average power not only stops increasing but also decreases.

On the contrary, as shown empirically, the IC-based circuit does not show the same performance, and it is the most efficient among all the circuits under test compared here. The reason behind the difference among the performance of the electronic circuits under test is explained next, where the efficiency of the electronic circuits with multiple harvesters is analyzed.

5. Efficiency analysis of the electronic circuits with multiple harvesters

As a rule, ideally, when two EH circuits are connected in parallel, it is expected that the amount of total transferred power is equal to the sum of the power transferred by each single circuit. However, the tests demonstrated that the diode full-bridge rectifier, series SSHI and SECE EH circuits lose efficiency when same circuits are added in parallel. The loss of efficiency is intrinsic to the circuit and independent from the vibratory energy source.

Some authors use different topologies to connect multiple harvesting circuits with the purpose of minimizing the efficiency loss. For instance, Boisseau et al. [37] introduced a harvester for multiple transducers based on a SECE circuit where the output stage is implemented with a single flyback converter. On the other hand, Romani et al. [38] implemented a harvester for multiple transducers based on a SECE circuit, with a single shared inductor and capacitor combined with a passive interface, to allow collect energy under low levels of input voltages. In both cases, each transducer is accompanied by its corresponding diode full-bridge rectifier, the switch to connect to the output converter and its respective control and drive circuits for the switch. In some cases one more diode to prevent reverse flowing of the current between circuits is added.

But if no components are added to the basic schemes shown in Figure 6(b) and Figure 6(c), the loss of efficiency takes place. The loss is due to the operation procedure of the EH circuits. SSHI and SECE circuits are divided into two stages: the first one harvest the energy from the vibratory source

Preprints (www.preprints.org) | NOT PEER-REVIEWED | Posted: 17 March 2017 doi:10.20944/preprints201703.0140.v1

and the second one gets the energy from the capacitor. When several circuits are connected and share the energy transfer stage, it is just a matter of probability to lose efficiency in the energy transfer or find saturation in some component. In the SECE circuit, it is likely to find saturation in the shared inductor because of the excess of instant current when two or more harvesters transfer energy at the same time. In the SSHI circuit, there is feedback of part of the output current towards some of the harvesting circuits.

In order to analyze the performance of each type of circuit, the currents that charged the store capacitor were measured when one or several circuits were connected in parallel. To ease the measurement, a shunt resistor of 1 ohm was connected between then energy management circuit output and the store capacitor. The measurement of the capacitor charging current allows to know the amount of the total charge transferred and allows the quantification of the efficiency of each type of EH circuit when the amount of circuits in parallel is increased.

In the basic SECE EH circuit, there is a way to ensure that all the interconnected circuits transfer the harvested charge at their maximum, as introduced in [37], and avoid the problem of unsynchronized discharge to the output stage.

In the series SSHI circuit, each one included its own independent switch circuit and inductor, as shown in Figure 6(b). During the tests, the input signals were also interconnected. Therefore, the linearity of the multi-harvester EH circuit could be tested, i.e., it could be checked if two circuits transferred twice the charge of a single circuit.

Figure 13 shows the results of the tests with series SSHI circuits in two situations: with a single circuit, and with two circuits. The waveforms represent the short interval where the source voltage is inverted as a result of the switching process. During this interval a resonant circuit is formed and the current is transferred from input source to store capacitor. The screen captured in Figure 13 shows the measure of the current average value during the 250 μs interval. This measure indicates the amount of charge transferred to the capacitor. Comparing the average values of the charging current for a single circuit and for two circuits, 54.4 and 98.4 mA respectively, a 10% efficiency loss can be seen. In fact, Figure 12 shows that the efficiency loss increases when operating with more circuits in parallel.

As a result of the graphical examination of Figure 13, three time intervals can be distinguished: T1, T2, and T3. As it can be seen, T1 and T3 intervals show a smaller slope than T2 interval. The slopes are different because there is magnetic saturation in the inductor and, hence, its inductance decreases, when the current reaches 100 mA. The current peak value increases from 432 mA, with a single circuit, to 672 mA, with two circuits. The value is smaller than the double of a single circuit, 860 mA, and, therefore, it is a fact that the switching process in the two circuits is not synchronized. The inductors used in the tests (Coilcraft's LPS6235 low profile series, 6x6x3 mm size) exhibit an inductance range from 1 mH to 10 mH with saturation currents ranging from 200 mA to 70 mA, respectively.

The results in the SECE EH circuit are analogous to the ones in the series SSHI circuit, already explained. The SECE circuits, when connected in parallel, share the inductor. Therefore, the probability of saturation is increased, particularly when the current from each circuit is discharged simultaneously onto the inductor.

Preprints (www.preprints.org) | NOT PEER-REVIEWED | Posted: 17 March 2017 doi:10.20944/preprints201703.0140.v1

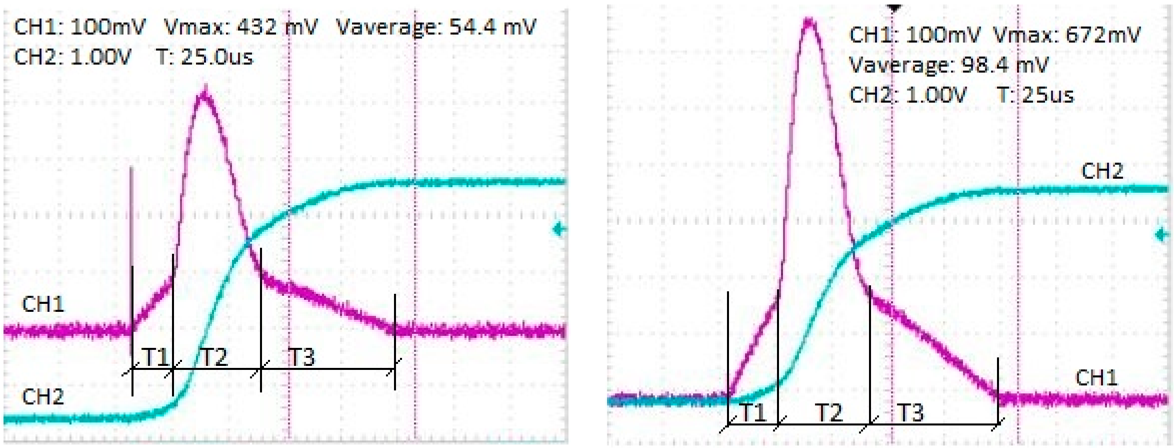

(a) (b)

Figure 13. Oscilloscope screen captures that show the input voltage from the energy source (CH2), and the output current (CH3). The signal in CH3 is the voltage measured in the 1 ohm shunt resistor, so mV corresponds to mA. (a) Single series SSHI EH circuit. (b) Two series SSHI EH circuits.

On the other hand, the IC-based circuit features a regulated maximum output current, which maintains a constant peak current value. Such maximum output current is extremely useful when working with various integrated circuits in parallel.

This IC includes three stages: the first one, the middle and the output stages. In the first one, the piezoelectric electrodes are connected to a low-loss full-wave bridge rectifier with a high-efficiency buck converter. This stage forms a complete energy harvesting system that is optimized for high-output impedance energy sources, such as piezoelectric transducers. The middle and output stages are inactive while the input capacitor gets charge, i.e., until the input voltage is greater than a fixed upper threshold. This way, the consumption of the system is reduced. When the input is above the threshold, the internal circuitry wakes up and the buck converter transfers efficiently a portion of the stored charge to the output. After the transfer, the input voltage decreases to the specified lower threshold voltage in the sleep state. When in sleep, both the input and output quiescent currents are minimal.

The reason for such high efficiency is that the output stage converter in IC-based circuit is decoupled from the input stage and it always operates under the same current and voltage conditions (amplitude and frequency). In fact, even if more energy sources are added, the output current in the IC-based circuit keeps its peak value.

Figure 14 shows the current burst waveforms while the store capacitor gets charged for both situations, with a single IC-based EH circuit, and with four IC-based circuits operating simultaneously. The duration of this time interval is 1.88 ms in the first case, and 7.5 ms in the last one. Moreover, the maximum amplitude of the current burst is constant in both cases. It means that the amount of transferred charge when four circuits are operating in parallel is almost four times the charge transferred by the operation of a single circuit.

Preprints (www.preprints.org) | NOT PEER-REVIEWED | Posted: 17 March 2017 doi:10.20944/preprints201703.0140.v1

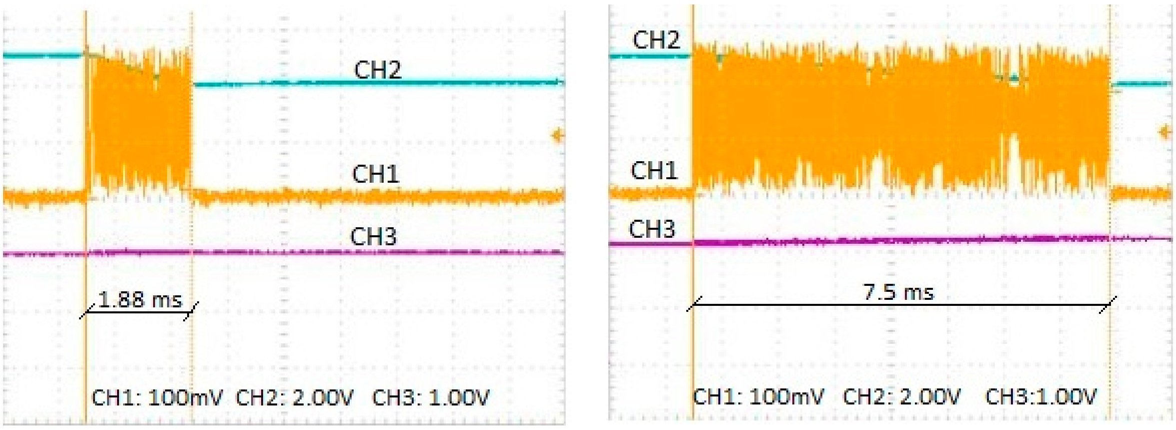

(**a**) (**b**)

Figure 14. Operation of the IC-based EH circuit. (a) a single circuit. (b) four circuits in parallel. The CH1 waveform shows the output current burst measured in the store capacitor. The CH2 shows the voltage decrease in the rectifying capacitor. The CH3 shows the voltage increase in the store capacitor.

So, not only the procedure of the tests was validated but also it was demonstrated that the IC-based EH circuit shows the best features to operate in a multi-harvester. In fact, the total amount of the harvested energy by a multi-harvester IC-based EH circuit is almost the sum of the energy harvested by each one of the harvester circuits. Therefore, it can be stated that the amount of energy collected by the IC-based multi-harvester is practically the one that could be collected in the ideal situation.

6. Conclusions

Monitoring systems require some kind of power supply, and their power requirements are usually satisfied through the connection to the electric power supply. Unfortunately, sometimes the monitoring systems do not have the chance to be connected to the electric power supply. On the other hand, the breakthroughs in technology make such systems need less power than in the past. Nowadays, EH systems can satisfy these requirements and can be considered as a plausible solution for the deployment of monitoring systems. However, using only one vibration based source of energy in the EH system is not enough to satisfy the power requirements in many monitoring applications.

The paper focuses on increasing the efficiency of vibration based EH circuits with multiple energy harvesters. As a result, the application range of such EH systems is enlarged. Then, here the use of multi-harvesters is considered, and, hence, some single EH systems are interconnected to supply more power to, for example, a monitoring system.

Some currently state-of-the-art EH circuits are analyzed in this paper. As the amount of circuits connected in parallel grows, the slope of the actual average power harvested with SECE or series SSHI circuits connected in parallel shows a certain decrease from the theoretical linear value.

On the contrary, it is demonstrated that the IC-based EH-circuit shows the best features to operate in a multi-harvester circuit, i.e., it is fully scalable and, therefore, it is the most suitable and efficient circuit to build a multi-harvester EH system. This feature is the most important one and it makes the multi-harvester strategy outstanding.

References

1. Erturk, A.; Inman, D. J. *Piezoelectric energy harvesting*. John Wiley & Sons, 2011.
2. Mitcheson, P. D.; Yeatman, E. M.; Rao, G. K.; Holmes, A. S.; Green, T. C. Energy harvesting from human and machine motion for wireless electronic devices. *Proceedings of the IEEE* **2008**, vol. 96, no. 9, pp. 1457–1486.

3. Beeby, S. P.; Tudor, M. J.; White, N. M. Energy harvesting vibration sources for microsystems applications. *Measurement Science and Technology* **2006**, vol. 17, p. R175.
4. Zhang, Q.; Kim, E. S. Vibration energy harvesting based on magnet and coil arrays for watt-level handheld power source. *Proceedings of the IEEE* **2014**, vol. 102, no. 11, pp. 1747-1762.
5. Wischke, M.; Masur, M.; Goldschmidtboeing, F.; Woias, P. Electromagnetic vibration harvester with piezoelectrically tunable resonance frequency. *Journal of Micromechanics and Microengineering* **2010**, vol 20, no. 3, pp. 035025.
6. Wang, F.; Hansen, O. Electrostatic energy harvesting device with out-of-the-plane gap closing scheme, *Sensors and Actuators A: Physical* **2014**, vol. 211, pp. 131–137.
7. Crovetto, A.; Wang, F.; Hansen, O. Modeling and optimization of an electrostatic energy harvesting device. *IEEE/ASME Journal of Microelectromechanical Systems* **2014**, vol. 23, no. 5, pp. 1141-1155.
8. Suzuki, Y. Recent progress in MEMS electret generator for energy harvesting. *IEEJ Transactions on Electrical and Electronic Engineering* **2011**, vol. 6, no. 2, pp. 101–111.
9. Li, S.; Crovetto, A.; Peng, Z.; Zhang, A.; Hansen, O.; Wang, M.; Li, X.; Wang, F. Bi-resonant structure with piezoelectric PVDF films for energy harvesting from random vibration sources at low frequency. *Sensors and Actuators A: Physical* **2016**, vol. 247, pp. 547–554.
10. Li, S.; Peng, Z.; Zhang, A.; Wang, F. Dual resonant structure for energy harvesting from random vibration sources at low frequency. *AIP Advances* 6 **2016**, pp. 015019.
11. Xu, R.; Lei, A.; Dahl-Petersen, C.; Hansen, K.; Guizzetti, M.; Birkelund, K.; et al. Screen printed PZT/PZT thick film bimorph MEMS cantilever device for vibration energy harvesting. *Sensors and Actuators A: Physical* **2012**, vol. 188, pp. 383–388.
12. Perpetuum. Available online: www.perpetuum.co.uk (accessed on 11 July 2016).
13. Wang, F.; Hansen, O. Invisible surface charge pattern on inorganic electrets. *IEEE Electron Device Letters* **2013**, vol. 34, no. 8, pp. 1047-1049.
14. Wang, F.; Bertelsen, C.; Skands, G.; Pedersen, T.; Hansen, O. Reactive ion etching of polymer materials for an energy harvesting device. *Microelectronics Engineering* **2012**, vol 97, pp. 227–230.
15. Lo H.; Tai, Y.-C. Parylene-based electret power generators. *Journal of Micromechanics and Microengineering* **2008**, vol. 18, no. 10, pp. 104006-1–104006-8.
16. Ferro solutions. Available online: www.ferrosi.com (accessed on 11 July 2016).
17. Miao, P.; Mitcheson, P.D.; Holmes, A. S.; Yeatman, E. M.; Green, T. C. Micro-Machined Variable Capacitors for Power Generation, *Conference Series-Institute of Physics* **2006**, vol. 178, pp. 53-58. Philadelphia; Institute of Physics; 1999.
18. Despesse, J.; Chaillout, T. F.; Cardot, A. Innovative structure for mechanical energy harvesting. International conference on solid–state sensors, actuators and Microsystems. *Transducers* **2007**, pp. 895–8.
19. Roundy, S.; Wright, P. K. A piezoelectric vibration based generator for wireless electronics. *Smart Mater. Struct.* **2004**, vol. 13, no. 5, pp. 1131– 142.
20. Elfrink, R.; Kamel, T.; Goedbloed, M.; Matova, S.; Hohlfeld, D.; Van Schaijk, R. Vibration energy harvesting with aluminum nitride-based piezoelectric devices. *Proceedings of the power MEMS workshop* **2008**, pp. 249–52.
21. Mehraeen, S.; Jagannathan, S.; Corzine, K. Energy harvesting from vibration with alternate scavenging circuitry and tapered cantilever beam. *IEEE Trans. Ind. Electron.* **2010**, vol. 57, pp. 820–830.
22. Karami, M. A.; Inman, D. J. Electromechanical modeling of the low-frequency zigzag micro-energy harvester. *J. Intell. Mater. Syst. Struct.* **2011**, vol. 22, pp. 271–282..
23. Berdy, D. F.; Srisungsitthisunti, P.; Jung, B.; Xu, X.; Rhoads, J.; Peroulis, D. Low-Frequency Meandering Piezoelectric Vibration Energy Harvester. *IEEE Trans. Ultrason. Ferroelectr. Freq. Control* **2012**, vol. 59, pp. 846–858.
24. Hu, A.; Xue, H.; Hu, H. Broadband Piezoelectric Energy Harvesting Devices Using Multiple Bimorphs with Different Operating Frequencies. *IEEE Trans. Ultrason. Ferroelectr. Freq. Control* **2008**, vol. 55, pp. 524-535.
25. Wang, W.; Yang, T. Q.; Chen, R.; Yao X. Vibration Energy Harvesting Using a Piezoelectric Circular Diaphragm Array. *IEEE Trans. Ultrason. Ferroelectr. Freq. Control* **2012**, vol. 59, 9, pp. 584–595.
26. Kubba, A.; Jiang, K. Efficiency Enhancement of a Cantilever-Based Vibration Energy Harvester, *Sensors,* **2014**, vol. 14, pp. 188-211.

27. Burrow, S. G.; Mitcheson, P. D.; Stark, B. H. Power Conditioning Techniques for Energy Harvesting. In *Advances in Energy Harvesting Methods*; Elvin, N., Erturk, A.; Springer, 2013.
28. Tabesh, A.; Fréchette, L. G. A Low-Power Stand-Alone Adaptive Circuit for Harvesting Energy From a Piezoelectric Micropower Generator, *IEEE Trans. Ind. Electron*.,**2010**, 57, 3,pp 625-637.
29. Ottman, G. K.; Hofmann, H. F.; Lesieutre, G. A. Optimized piezoelectric energy harvesting circuit using step-down converter in discontinuous conduction mode, *IEEE Trans. Power Electron*., **2003**, 18, 2, pp. 696–703.
30. Lefeuvre, E.; Audigier, D.; Richard, C.; Guyomar, D. Buck boost converter for sensorless power optimization of piezoelectric energy harvester, *IEEE Trans. Power Electron*., **2007**, 22, 5, pp. 2018–2025.
31. Yu, H.; Zhou, J.; Deng, L.; Wen, Z. A Vibration-Based MEMS Piezoelectric Energy Harvester and Power Conditioning Circuit, *Sensors*, **2014**, 14, pp. 3323-3341.
32. Chao, L.; Raghunathan, V.; Roy, K. Efficient Design of Micro-Scale Energy Harvesting Systems, *IEEE Journal on Emerging and Selected topics in Circuits and Syste*ms, **2011**, 1, 3, pp. 254–266.
33. Linear Technologies. Available online: www.linear.com/product/LTC3588-1 (accessed on 12 December 2016).
34. Lin, H. C.; Wu, P. H.; Lien, I. C.; Shu, Y. C. Analysis of an array of piezoelectric energy harvesters connected in series, *Smart Materials and Structures*, **2013**, *22*, 9, 094026.
35. Smart Material. Available online: www.smart-material.com/MFC-product-main.html (accessed on 12 December 2016).
36. PSIM simulation software. Available online: powersimtech.com/ (accessed on 12 December 2016).
37. Boisseau, S.; Gasnier, P.; Perez, M.; Bouvard, C.; Geisler, M.; Duret, A. B.; Despesse, G.; Willemin, J. Synchronous Electric Charge Extraction for multiple piezoelectric energy harvesters. Proceedings of the IEEE 13th International New Circuits and Systems Conference (NEWCAS), Grenoble, France.

Romani, A.; Filippi, M.; Tartagni, M. Micropower design of a fully autonomous energy harvesting circuit for arrays of piezoelectric transducers, *IEEE Transactions on Power Electronics*, **2014**, 29, 2, pp. 729-739.